

Preparation and Structural Characterization of Polymer-Supported Methylrhenium Trioxide Systems as Efficient and Selective Catalysts for the Epoxidation of Olefins

Raffaele Saladino,^{*,†} Veronica Neri,[†] Anna Rita Pelliccia,[†] Ruggero Caminiti,[‡] and Claudia Sadun[‡]

Dipartimento A.B.A.C. Istituto Nazionale di Fisica della Materia, Università della Tuscia, Via S. Camillo de Lellis s.n.c., 01100, Viterbo, Italy, and Dipartimento di Chimica, Istituto Nazionale di Fisica della Materia, Università degli studi di Roma "La Sapienza", p.le Aldo Moro 5, 00185 Rome, Italy

saladino@unitus.it

Received October 29, 2001

Novel heterogeneous compounds of methylrhenium trioxide (MTO) were prepared with poly(4-vinylpyridine) and polystyrene as polymeric supports. The wide-angle X-ray diffraction (WAXS.) analysis, performed by the application of the *difference method*, showed, in a representative case of the poly(4-vinylpyridine)/MTO derivatives, a slightly distorted octahedral conformation on the metal's primary coordination sphere. The Re–O and Re–C bond distances were not influenced by the polymeric nature of the ligand, while the Re–N bond distance was abnormally shorter than those previously observed for homogeneous MTO/ L_n complexes, showing a strong coordination of the rhenium atom to the support. A set of scanning electron microscopy (SEM) photographs showing the morphology of the surface of particles of poly(4-vinylpyridine)/MTO and polystyrene/MTO systems are reported. The reticulation grade of the polymer was a crucial factor for the morphology of the particles surface. Poly(4-vinylpyridine) 2% cross-linked systems were characterized by particles with very irregular shape and surface. Poly(4-vinylpyridine) 25% cross-linked systems showed particles with regular spherical shape, which morphology was similar to microcapsules obtained with polystyrene. All novel MTO compounds were efficient and selective heterogeneous catalysts for the epoxidation of olefins using environmentally friendly H_2O_2 as oxygen atom donor. The catalyst activity was maintained for at least five recycling experiments.

Introduction

In the past few years methylrhenium trioxide (CH_3ReO_3 , MTO)¹ has become an important catalyst for its high efficiency and selectivity in a variety of synthetic transformations.² The advantages of MTO in oxidative reactions have been well-documented in the oxidation of olefins,³ alkynes,⁴ aromatic derivatives,⁵ sulfur compounds,⁶ phosphines,⁷ organonitrogen compounds,⁸ Baeyer–Villiger rearrangement,⁹ and oxygen

insertion into C–H bonds.¹⁰ Among them, the epoxidation of olefins has been extensively studied.¹¹ The role of MTO in these oxidations has been understood by the characterization of its reaction products with hydrogen peroxide (H_2O_2). The active catalytic forms are a mono-peroxo metal [$MeRe(O)_2(O_2)$] (**I**) and a bisperoxo metal [$MeRe(O)(O_2)_2$] (**II**) complexes and/or their adducts with solvent molecules.¹² A detailed structure of the 1:1 (**II**)/ H_2O /diglyme (diethylene glycol dimethyl ether) adduct, in which two η^2 -coordinated peroxo ligands are nearly coplanar with the Re–C bond, has been rigorously established by single-crystal X-ray analysis.¹² Theoretical studies have been performed to elucidate the reactivity of **I** and **II** toward olefins and the geometrical features of the transition state of the epoxidation.¹³

Although effective for numerous substrates, the most important drawback of this reaction is the concomitant ring opening of the oxiranyl ring to form *trans*-1,2-diols.¹⁴

* Corresponding author. Phone 39(0)761357284. Fax 39(0)761357242.

[†] Università della Tuscia.

[‡] Università degli studi di Roma "La Sapienza".

(1) Beattie, I. R.; Jones, P. J. *Inorg. Chem.* **1979**, *18*, 2318.

(2) Romão C. C.; Kühn, F. E.; Herrmann W. A. *Chem. Rev.* **1997**, *97*, 3197–3246.

(3) Herrmann W. A.; Fischer, R. W.; Marz, D. W. *Angew. Chem., Int. Ed. Engl.* **1991**, *30*, 1638.

(4) Zhu, Z.; Espenson, J. H. *J. Org. Chem.* **1995**, *60*, 7728.

(5) (a) Adam, W.; Herrmann W. A.; Lin J.; Saha-Moller C. R. *J. Org. Chem.* **1994**, *59*, 8281–8283. (b) Adam, W.; Herrmann W. A.; Lin J.; Saha-Moller C. R.; Fischer, R. W.; Correia, J. D. G. *Angew. Chem., Int. Ed. Engl.* **1994**, *33*, 2475–2477. (c) Adam, W.; Herrmann W. A.; Saha-Moller C. R.; Shimizu M. *J. Mol. Catal. A.* **1995**, *97*, 15–20. (d) Saladino, R.; Neri, V.; Mincione, E.; Marini, S.; Coletta, M.; Fiorucci, C.; Filippone, P. *J. Chem. Soc., Perkin Trans. 1* **2000**, 581–586.

(6) (a) Huston, P.; Espenson, J. H.; Bakac, A. *Inorg. Chem.* **1993**, *32*, 4517. (b) Brown, K. N.; Espenson, J. H. *Inorg. Chem.* **1996**, *35*, 7211.

(7) Abu-Omar, M. M.; Espenson, J. H. *J. Am. Chem. Soc.* **1995**, *117*, 272.

(8) (a) Zhu, Z.; Espenson, J. H. *J. Org. Chem.* **1995**, *60*, 1326. (b) Murray, R. W.; Iyanar, K.; Chen, J.; Wearing, J. T. *Tetrahedron Lett.* **1996**, *37*, 805–808. (c) Goti, A.; Nannelli, L. *Tetrahedron Lett.* **1996**, *37*, 6025–6028.

(9) (a) Herrmann W. A.; Fischer, R. W.; Correia, J. D. G. *J. Mol. Catal.* **1994**, *94*, 213–223. (b) Bernini, R.; Mincione, E.; Cortese, M.; Aliotta, G.; Saladino, R. *Tetrahedron Lett.* **2001**, *42/32*, 5401–5404.

(10) (a) Murray, R. W.; Iyanar, K.; Chen, J.; Wearing, J. T. *Tetrahedron Lett.* **1995**, *36*, 6415. (b) Schuchardt, U.; Mandelli, D.; Shul'pin, G. B. *Tetrahedron Lett.* **1996**, *37*, 6487–6490.

(11) Al-Ajlouni, A. M.; Espenson, J. H. *J. Org. Chem.* **1996**, *61*, 3969–3976.

(12) Herrmann W. A.; Fischer, R. W.; Scherer, W.; Rauch, M. U. *Angew. Chem., Int. Ed. Engl.* **1993**, *32*, 1157–1160.

(13) (a) Wu, Y.-D.; Sun, J. *J. Org. Chem.* **1998**, *63*, 1752–1753. (b) Gisdakis, P.; Antonczak, S.; Köstlmeier, S.; Herrmann W. A.; Rösch, N. *Angew. Chem., Int. Ed.* **1998**, *37*, 2211.

Two general procedures have been developed to avoid this problem. The first procedure requires an anhydrous reaction medium, which is usually obtained by the use of nonaqueous media and dried H₂O₂ in *tert*-butyl alcohol,³ or urea/hydrogen peroxide adduct (UHP) in CH₂Cl₂.¹⁵ In the case of UHP, the helical urea channels may serve as an host confined stabilizing environment for MTO.¹⁶ Recently, the MTO/UHP protocol has been applied for the synthesis of sensitive 5,6-oxiranyl-5,6-dihydrouracils, which are of particular biological significance because responsible for the formation of protein–nucleic acids cross-links.¹⁷ The second procedure requires the use of low molecular weight compounds bearing one or more nitrogen atoms as mediators of the oxidation.¹⁸ Lewis base adducts of MTO, of general formula MTO/L_{*n*} (where L = ligand, *n* = 1 or 2), prepared by reaction with pyridine,¹⁹ pyridine derivatives,²⁰ quinuclidine,²¹ aniline, toluidine, and pyrazole,²² decrease the formation of diols mainly as a consequence of the reduced Brønsted and Lewis acidity of the catalyst system. The structures of these MTO/L_{*n*} complexes have been characterized by means of single-crystal X-ray, neutron, or electron diffraction. All show a slightly distorted tetrahedral geometry with the methyl group and the ligand in a *trans*-configuration to each other in the apical positions.^{2,22} Moreover, it was found that a biphasic system and excess of pyridine not only prevent the formation of diols but also increase the reaction rate in comparison to MTO.^{19,23}

Herrmann and co-workers extended in a patent²⁴ the “mediator” concept by the preparation of heterogeneous MTO compounds, of general formula (polymer)_{*f*}/(MTO)_{*g*} (the *fg* quotient expresses the ratio by weight of the two components), in which MTO was supposed to be bonded to the support by coordination with only one nitrogen atom in analogy with the homogeneous systems. Unreticulated poly(4-vinylpyridine), poly(2-vinylpyridine), poly(vinylpyrrolidone), poly(acrylamide), and nylon 6 were used as organic supports. The heterogeneous rhenium compounds were applied for the epoxidation of cyclohexene, methyl oleate, and allyl alcohol with dried H₂O₂ in *tert*-butyl alcohol. Unfortunately, low yields of cyclohexene oxide and 1,2-epoxypropane-3-ol (27% and 20%, respectively) were obtained.²⁴ The structures of these (polymer)_{*f*}/(MTO)_{*g*} systems were not completely characterized (only the elemental analysis was reported), and useful structure activity relationships are still lacking.

Apart from a silica supported MTO complex of γ -(2,2'-dipyridyl)aminopropylpolysiloxane,²⁵ and a NaY zeolite/MTO supercage system,²⁶ no further data are available in the literature about heterogeneous MTO catalysts. The heterogeneization of MTO by using a polymeric support is an important tool because it allows an easier recovery of the catalyst and, sometimes, may improve the reactivity.²⁷

We report here the preparation of a novel family of poly(4-vinylpyridine)/MTO systems by the use of poly(4-vinylpyridine) 25% cross-linked (with divinylbenzene) (PVP-25%), and poly(4-vinylpyridine-*N*-oxide) 2% cross-linked (PVPN-2%) as supports. Poly(4-vinylpyridine) 2% cross-linked (PVP-2%) was also used as a reference system. Since the reactivity of polymer catalysts having coordinate bonds can be low, an unprecedented preparation of microencapsulated MTO,²⁸ with polystyrene 2% cross-linked (with divinylbenzene) (PS-2%) or a mixture of PS-2% and PVP-2% (optimal ratio 5:1), is also studied. The novel (polymer)_{*f*}/(MTO)_{*g*} systems have been characterized by infrared spectroscopy and scanning electron microscopy (SEM). In a representative case, the PVP-2%/MTO complex, a detailed structure of the local geometry of the rhenium atom was obtained for the first time by an Energy-Dispersive X-ray diffraction (EDXD) analysis. The PVP-2%/MTO, PVP-25%/MTO, PVPN-2%/MTO, and PS-2%/MTO catalysts have been used for the efficient and selective epoxidation of olefins with H₂O₂ (35% water solution) as environmentally friendly oxidant. The role on the reaction pathway of several parameters, such as the loading factor, the reticulation grade of the support, the shape and dimension of particles, the coordinate versus coating immobilization, and the nature of the heterogeneous atom bonded to rhenium, is also described.

Preparation and Characterization of Poly(4-vinylpyridine)/MTO and Polystyrene/MTO Catalyst Systems. PVP-2% **1**, PVP-25% **2**, and PS-2% **7** were obtained from a commercial source (Aldrich). PVPN-2% **3** was obtained by oxidation of **1** with an excess of 3-chloroperbenzoic acid (*m*-CPBA) in ethanol (EtOH) at room temperature.²⁹ The preparation of PVP-2%/MTO **4**, PVP-25%/MTO **5**, and PVPN-2%/MTO **6** complexes was performed by a modification of the procedure described by Herrmann.²⁴ Compounds **1**, **2**, **3** were suspended in ethanol at room temperature, and to these solutions was added the appropriate amount of powdered MTO under nitrogen atmosphere (as represented in the schematic drawing in Scheme 1).

The mixture was stirred for 1 h at room temperature and then cooled to 0 °C. During this period polymers changed from colorless to bright yellow, with the exception of **3** that shows only a weak color. The mixture was filtered and the solid residue washed with ethyl acetate several times. No traces of MTO were found in the organic phase. Under otherwise specified, poly(4-vinylpyridine)/MTO complexes were prepared with a loading factor (that is mmol of MTO for 1 g of support)

(14) Gansäuer, A. *Angew. Chem., Int. Ed. Engl.* **1997**, *36*, 2591–2592.

(15) Adam, W.; Mitchell, C. M. *Angew. Chem., Int. Ed. Engl.* **1996**, *35*, 533–535.

(16) Adam, W.; Mitchell, C. M.; Saha-Moller, C. R.; Weichold, O. *J. Am. Chem. Soc.* **1999**, *121*, 2097–2103.

(17) Saladino, R.; Carlucci, P.; Danti, M. C.; Crestini, C.; Mincione, E. *Tetrahedron* **2000**, *56*, 10031–10037.

(18) Herrmann, W. A.; Fischer, R. W.; Rauch, M. U.; Scherer, W. *J. Mol. Catal.* **1994**, *86*, 243–266.

(19) Herrmann, W. A.; Kühn, F. E.; Mattner, M. R.; Artus, G. R. J.; Geisberger, M.; Correia, J. D. G. *J. Organomet. Chem.* **1997**, *538*, 203.

(20) (a) Copèret, C.; Adolffson, H.; Sharpless, K. B. *J. Chem. Soc., Chem. Commun.* **1997**, 1915. (b) Herrmann, W. A.; Kratzer, R. M.; Ding, H.; Glas, H.; Thiel, W. R. *J. Organomet. Chem.* **1998**, *555*, 293.

(21) Herrmann, W. A.; Correia, J. D. G.; Rauch, M. U.; Artus, G. R.; Kühn, F. E. *J. Mol. Catal.* **1997**, *118*, 33.

(22) Kühn, F. E.; Santos, A. M.; Roesky, P. W.; Herdtweck, E.; Scherer, W.; Gisdakis, P.; Yudanov, I. V.; Di Valentin, C.; Röscher, N. *Chem. Eur. J.* **1999**, *5*, 3603–3615.

(23) Rudolph, J.; Reddy, K. L.; Chiang, J. P.; Sharpless, K. B. *J. Am. Chem. Soc.* **1997**, *119*, 6189.

(24) Herrmann, W. A.; Fritz-Meyer-Weg, D. M.; Wagner, M.; Kuchler, J. G.; Weichselbaumer, G.; Fischer, R. U.S. Patent 5,155,247 (Oct. 13, 1992).

(25) Wang, T.-J.; Li D.-C.; Bai, J.-H.; Huang, M.-Y.; Jiang, Y.-Y. *J. Macromol. Sci., Pure Appl. Chem.* **1998**, *A35*, 531–538.

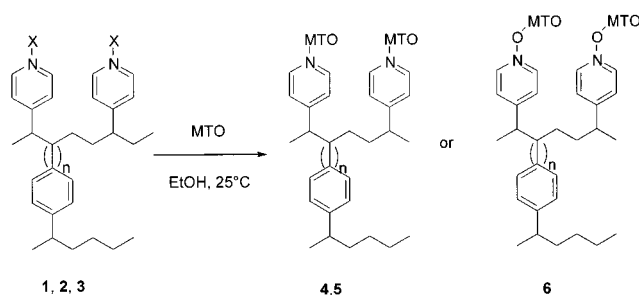
(26) Adam, W.; Saha-Möller, C. R.; Weichold, O. *J. Org. Chem.* **2000**, *65*, 2897–2899.

(27) Thomas, J. M.; Thomas W. J. *Principles and Practice of heterogeneous catalysis*; VCH: New York, 1997.

(28) Donbrow, M. *Microcapsules and Nanoparticles in Medicine and Pharmacy*; CRC Press: Boca Raton, FL, 1992.

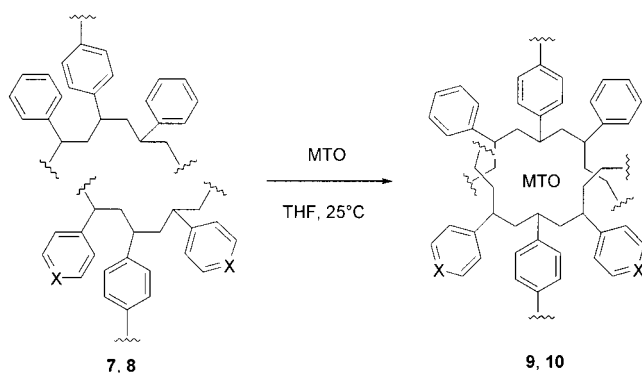
(29) Ochiai, E. *Aromatic Amine Oxides*; Elsevier: Amsterdam, 1967.

Scheme 1



1, 4: X= lone pair; n= 2% cross-linked. 2, 5: X= lone pair; n= 25% cross-linked. 3: X= oxygen; n= 2% cross-linked. 6: n=25% cross-linked.

Scheme 2



7, 9: X=CH; n= 2% cross-linked. 8, 10: X= nitrogen; n= 2% cross-linked.

equal to 0.5. Compounds **4**, **5**, and **6** were used without any further purification. The preparation of PS-2%/MTO **9** and PS-2%/PVP-2%/MTO **10** was performed by the microencapsulation technique.²⁸ Polystyrene microcapsules have been used for coating and isolating Lewis acids on the basis of physical envelopment by the polymer and on electron interactions between the π electrons of the benzene ring and the metal center.³⁰ The size of microcapsule achievable has been reduced from a few micrometers to nanometers.²⁸ Compound **7**, or a mixture of **7** and **1** (ratio **7:1** = 5:1), namely compound **8**, was suspended at room temperature in tetrahydrofuran (THF, 5 mL), which is a solvent with high swelling properties toward polystyrene (9.9 cal cm⁻³).³¹ Under these experimental conditions MTO might enter the enlarged mesh structure of the polymer. To this mixture the appropriate amount of powdered MTO was added as a solid core under nitrogen atmosphere at room temperature (as represented in the schematic drawing in Scheme 2).

Grumes were found in suspension in the mixture, and hexane (10 mL) was added to harden the capsule walls. The mixture was stirred during 1 h, and in this period the mixture changed from colorless to bright blue. No traces of MTO were found in the organic phase after the workup of the reaction. The polystyrene/MTO microcapsules were prepared with a loading factor equal to 0.5. Compounds **9** and **10** were used without any further purification. Control experiment using polybutadiene or polyethylene as polymeric matrixes were performed. While 95% of MTO (100% = the amount of MTO microencapsulated on polystyrene) was immobilized by

Table 1. $\nu(\text{ReO})$ Vibrational Frequencies of PVP/MTO Complexes and PS/MTO Microcapsules^a

compound	$\nu(\text{ReO})$ cm ⁻¹
PVP-2%/MTO 4	963, 923
PVP-25%/MTO 5	964, 932
PVPN-2%/MTO 6	924
PS-2%/MTO 9	953, 911
PS-2%(PVP-2%)/MTO 10	960, 921

^a Data recovered for solid KBr samples at room temperature.

polybutadiene, only 11% of MTO was observed in the polyethylene system as revealed by elemental analysis.³²

FT-IR spectroscopy appeared to be a useful tool to evaluate the electronic properties of the ReO₃ fragment in poly(4-vinylpyridine)/MTO complexes and polystyrene/MTO microcapsules since the $\nu(\text{ReO})$ vibrational frequencies are highly characteristic of alkyltrioxorhenium (VII) compounds. On the basis of the theoretical valence-bond resonance structures for the Re–O bond, the $\nu(\text{ReO})$ vibration is expected to shift to lower frequencies in the presence of electron-donating ligands with respect to electron-withdrawing ligands.² The assignment of the vibration modes of the ReO₃ fragment in several R–ReO₃ and R–ReO₃/ligand(s) has been previously reported in the literature,³³ also by inelastic neutron scattering (INS) and high-resolution FT-Raman analyses.³⁴ To the best of our knowledge, there are no reports dealing with the FT-IR data of polymer-supported MTO systems. Table 1 gives the values recovered for $\nu(\text{ReO})$ stretching vibration frequencies of compounds **4**, **5**, **6**, **9**, and **10**, as revealed by solid-state FT-IR (KBr) analyses.

The $\nu(\text{ReO})$ frequencies of polymer-supported MTO systems display values that are lower than that found for MTO, equal to 998 cm⁻¹ for the symmetric stretching vibration mode, and 959 cm⁻¹, for the asymmetric stretching vibration mode.³⁴ These values are close to that reported for homogeneous low molecular weight MTO complexes. On the basis of these data it is reasonable to suggest that also in the case of polymer-supported MTO systems, the π -bonded hydrocarbon ligands and Lewis bases ligands lower the Re–O bond order, probably as a result of their electron-donating abilities. Moreover, compound **9** shows $\nu(\text{ReO})$ frequencies that are lower with respect to **4–6**, in accord with the order of increasing Re–O bond order previously described for Cp*ReO₃ (Cp* = cyclopentadienyl), MTO/bipyridine, PhReO₃, and free MTO.³⁵ PS-2%(PVP-2%)/MTO **10** displays an intermediate value.

A set of scanning electron microscopy (SEM) photographs showing the morphology of the surface of particles of poly(4-vinylpyridine)/MTO and polystyrene/MTO systems are reported in Figures 1–5. Compound **4** shows particles of different shapes, with very irregular surfaces, and characterized by a scaffold of an average size of the order of 100 μm (Figure 1). At a largest magnification,

(31) Polo, E.; Amadelli, R.; Parassiti, V.; Maldotti, A. *Inorg. Chim. Acta* **1992**, *192*, 1.

(32) Even if we have not studied in detail the oxidation state of the rhenium atom into microcapsules, the possibility of electron transfer processes to Re(VI), which is consistent with the blue color of the catalyst and with the significantly lower value of the R–O IR frequencies, cannot be completely ruled out.

(33) Mink, J.; Keresztury, G.; Stirling, A.; Herrmann, W. A. *Spectrosc. Chim. Acta* **1994**, *50A*, 2039.

(34) Parker, S. F.; Herman, H. *Spectrochimica Acta* **2000**, *56A*, 1123–1129.

(35) Herrmann, W. A.; Roesky, P. W.; Scherer, W.; Kleine, M. *Organometallics* **1994**, *13*, 4536.

(30) Kobayashi, S.; Nagayama, S. *J. Am. Chem. Soc.* **1998**, *120*, 2985–2986.

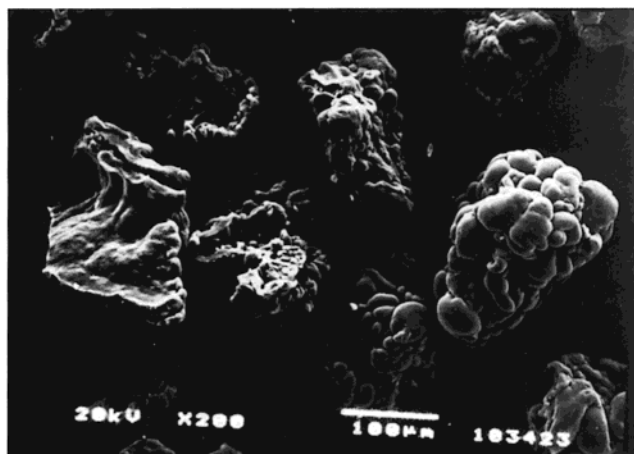


Figure 1. Scanning electron microscopy (SEM) micrograph of PVP-2%/MTO catalyst.

the surface appears defined by two different kinds of morphology: a partially fused smooth sheet-paving, and a chaotic aggregate of fusiform small “rounded-up” capsules adhered to each other, probably due to the small size of the core. Control experiments were performed with the aim to evaluate if the incorporation of MTO itself causes a change in the morphology of the polymer. The comparison between the electron microscopy photographs of **4** and PVP-2% alone not show appreciable differences. These data is in accord with the low value of the loading factor used in the preparation of the polymer.

A different morphology was observed for compound **5**. In this case, particles are characterized by a very regular spherical shape, with an average value of diameter of the order of 500 μm (Figure 2, panel a). A low number of irregular fragments was observed, which are probably formed by a mechanical damage of particles during the preparation of the sample. At a largest magnification the particles show a dense sheet paving, apparently formed by a compact aggregate of small grumes, which is partially covered by irregular craters. When a cross-section of particles was observed at large magnification, the core appeared to be formed by several superimposed layers, in which sheaves of fusiform fibers move from the center of particle to the surface. Channels, cavities, and small irregular grumes are distributed around and over the fibers (Figure 2, panel b).

The morphology of **6** appears to be similar to that previously observed for **4**. Particles are of different shapes, irregular surface, and with an average scaffold dimension of the order of 200 μm (Figure 3). Two main surface motifs are clearly evident; a compact and smooth sheet-paving and several “rounded-up” capsules partially fused on the sheet-paving of the particle.

As expected, compound **9**, which is a microencapsulated MTO system, is composed by regular spherical microcapsules, with an average value of diameter of the order of 100 μm (Figure 4). Also in this case, a low number of irregular fragments was observed.

Note that **10** is characterized by regular spherical microcapsules (Figure 5). Because of **4** shows particles of very irregular morphology, the spherical shape of particles of **10** is probably due to the efficient microencapsulation of the PVP-2% and MTO by PS-2%.

In the poly(4-vinylpyridine) family, a low value of the reticulation grade (2% cross-link with divinyl benzene) affords particles that are of different shapes and very

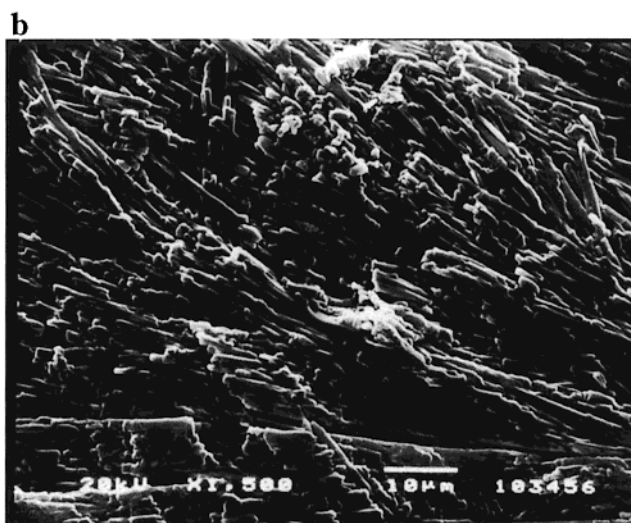


Figure 2. Panel a: Scanning electron microscopy (SEM) micrograph of PVP-25%/MTO catalyst. Panel b: cross-section at largest magnification.

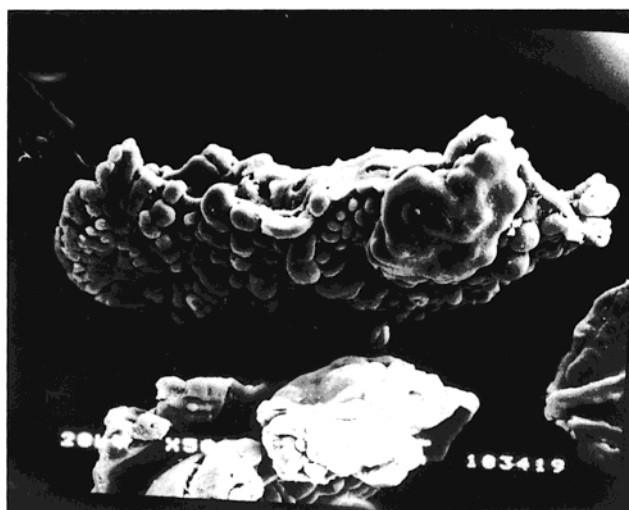


Figure 3. Scanning electron microscopy (SEM) micrograph of PVPN-2%/MTO catalyst.

irregular surfaces. In the presence of an increased value of the reticulation grade (25% cross-link with divinyl benzene), the transformation of irregular “spongy” particles to regular spherical particles is observed. Prelimi-

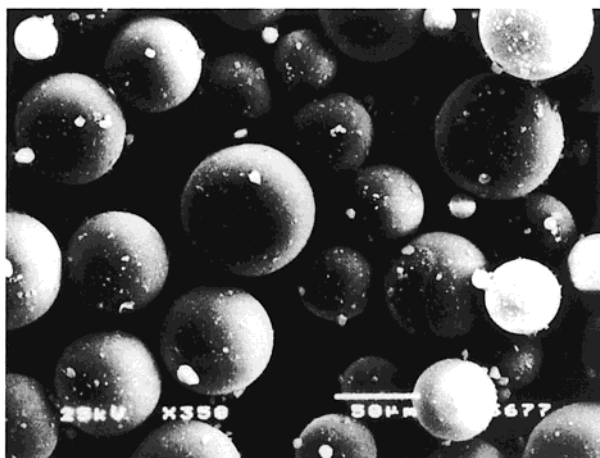


Figure 4. Scanning electron microscopy (SEM) micrograph of PS-2%/MTO catalyst.

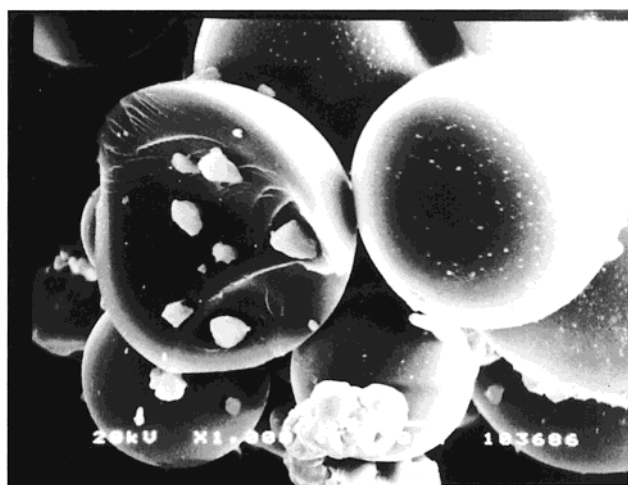


Figure 5. Scanning electron microscopy (SEM) micrograph of PS-2%/PVP-2%/MTO catalyst.

nary results obtained by an energy-dispersive X-ray (EDX) map of **4** showed that MTO is located efficiently over the polymer surface. Thus, it is reasonable to suggest that the polymer morphology may, at least in part, affect the behavior of the catalysts, mostly in the case of catalysts that are different only for the value of the reticulation grade. Polystyrene forms microcapsules that are characterized by an average value of the diameter that is smaller than that determined for the PVP-25%/MTO system. Finally, **10** microcapsules were obtained whatever the reticulation grade of the polyvinyl pyridine component.

Energy-Dispersive X-ray Diffraction Analysis. Wide-angle X-ray diffraction (WAXS) was used to determine the local geometry of the rhenium atom in compound **4**. This analysis is particularly well suited for providing insight into the way metal ions interact with their surroundings. The coordination geometry of several metal ions in amorphous state has been studied using this technique.^{36–38} The major difficulties in determining the coordination structure of a metal ion with a polymer system lie in its highly complex amorphous structure. Here we used the *difference method*,^{39,40} successfully

applied also to solid systems,⁴¹ for treating experimental WAXS data, assuming that polymer structure is not altered by methylrhenium trioxide (MTO) insertion, when **4** was prepared.

In this way, the radial distribution function of PVP-2%, the reference system, can be subtracted from the radial distribution function of **4**. By doing so, the contributions of MTO–polymer and MTO–MTO interactions remain.

The *difference method* of neutron diffraction and isotopic substitution (NDIS) has been applied by R. H. Tromp and G. W. Neilson⁴² to aqueous (D₂O) poly(styrene-sulfonate) ion-exchange resins with Ni(II) and Li(I).

The X-ray diffraction experiments were carried out with a noncommercial X-ray energy scanning diffractometer.^{43,44} The diffractometer consists of a Seifert X-ray generator equipped with a water-cooled tungsten X-ray source, with 3.0 kW maximum power. The *bremsstrahlung* component of the X-ray source was used. A Germanium solid-state detector (SSD) connected to a multichannel analyzer carried out the diffraction spectra collection by an electronic chain. A collimating system positioned in front of and behind the sample focuses the X-ray beam. Two-step motors for moving the arms supporting the source and the detector allow the angular positioning. An adjustable sample holder was used to position the sample in the optical center of the diffractometer.

The spectra were recorded at different fixed θ to obtain the complete q range. The function q can be written

$$q = 4\pi \sin \theta / \lambda = Ek \sin \theta$$

where q is expressed in (\AA^{-1}) and E in (keV), and the value of the constant k is 1.014.

Operating conditions were as follows: high voltage supply: = 50 kV, current = 35 mA, total power = 1750 W; energy range = 12.4 ÷ 50 keV; measurement angles (Θ) = 21.0°, 10.5°, 8.0°, 3.5°, 2.0°, 1.0°, 0.5°; scattering parameter range $q = 0.110 \div 16.0 \text{ \AA}^{-1}$.

It is necessary correct the experimental data^{45,46,47} normalizing to the incident radiation intensity and dividing by X-ray absorption and polarization coefficients. Other corrections are the escape peaks suppression and elimination of contributions due to the Mylar cell and inelastic scattering from the observed intensities $I(E, \Theta)$.

(37) Atzei, D.; De Filippo, D.; Rossi, A.; Caminiti, R.; Sadun, C. *Inorg. Chim. Acta* **1996**, *248* (2), 203.

(38) Atzei, D.; Sadun, C.; Pandolfi, L. *Spectrochimica Acta* **2000**, *56A*, 531.

(39) Gontrani, L.; Caminiti, R.; Bencivenni, L.; Sadun, C. *Chemical Phys. Lett.* **1999**, *301* (1–2), 131–137.

(40) Caminiti, R.; Carbone, M.; Panero, S.; Sadun, C. *J. Phys. Chem.* **1999**, *103* (4), 10348–10355.

(41) Atzei, D.; Ferri, T.; Sadun, C.; Sangiorgio, P.; Caminiti, R. *J. Am. Chem. Soc.* **2001**, *123* (11), 2552–2558.

(42) Tromp, R. H.; Neilson, G. W. *J. Phys. Chem.* **1996**, *100*, 7380–7383.

(43) (a) Caminiti, R.; Sadun, C.; Rossi, V.; Cilloco, F. Felici, R. Presented at the XXV Italian Congress on Physical Chemistry, Cagliari, Italy, 1991. (b) Caminiti, R.; Sadun, C.; Rossi, V.; Cilloco, F. Felici, R. Patent No. RM/93 01261484 June 23, 1993.

(44) Ballirano, P.; Caminiti, R.; Ercolani, C.; Maras, A.; Orrù, A. *J. Am. Chem. Soc.* **1998**, *120* (49), 12798–12807.

(45) Nishikawa, K.; Iijima, T. *Bull. Chem. Soc. Jpn.* **1984**, *57*, 1750.

(46) Fritsch, G.; Keimel, D. A. *Mater. Sci. Eng.* **1991**, *13A*, 888.

(47) Carbone, M.; Caminiti, R.; Sadun, C. *J. Mater. Chem.* **1996**, *6*, 1709.

(36) Atzei, D.; De Filippo, D.; Rossi, A.; Caminiti, R.; Sadun, C. *Spectrochimica Acta* **1995**, *51* (1) A, 11.

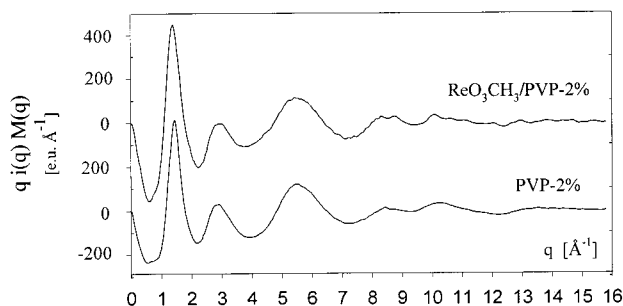


Figure 6. Experimental structure functions in the $qi(q)M(q)$ form: (a) $\text{ReO}_3\text{CH}_3/\text{PVP-2\%}$, (b) PVP-2\% .

Atomic scattering factors, $f_h(s)$, were taken from International Tables.⁴⁸ The static structure function

$$i(q) = I_{\text{coh}}(E) - \sum f_h^2(q)$$

was then calculated.

The radial distribution $D(r)$ is

$$D(r) = 4\pi r^2 \rho_0 + 2r\pi^{-1} \int_0^{S_{\text{max}}} qI(q)M(q)\sin(rq)dq$$

where q is the scattering parameter, ρ_0 the sample's average electronic density ($\rho_0 = (\sum_h m_h f_h(0))^2 V^{-1}$), V the stoichiometric unit volume chosen and $M(q)$ a modification function defined by

$$f_{\text{Re}}^2(0)/f_{\text{Re}}^2(q) \exp(-0.01q^2)$$

The experimental radial distribution functions are shown also as $\text{Diff}(r) = D(r) - 4\pi r^2 \rho_0$. Theoretical peaks were calculated by Fourier transformation of the theoretical intensities for the pair interactions,

$$i_{ij} = \sum f_i f_j \sin(r_{ij} q) (r_{ij} q)^{-1} \exp(-1/2\sigma_{ij}^2 q^2)$$

using the same sharpening function as for the experimental data and assuming the root-mean-square variation over distance to be σ_{ij} . The equipment and technique used are described in detail elsewhere.^{43,46}

The experimental structure functions show the typical behavior of an amorphous sample. The curves are very similar, exhibiting a similar oscillation period and amplitude. This suggests that the MTO inclusions do not modify the short-range order of polymer structure. The functions, in the range 0–16 \AA^{-1} , for PVP-2\% and **4**, are shown in Figure 6.

The experimental radial distribution function of PVP-2\% , in the $\text{Diff}(r)$ form, in the range 0–16 \AA (Figure 7) shows peaks at about 1.45 and 2.45 \AA and two large oscillations at greater distances.

The first peaks at 1.45 and 2.45 \AA can be attributed to interactions in the polymer molecule. They represent the distances between the directly bound atoms and between two nondirectly bound atoms. These nonbonded distances, like those between atoms 1–3 in the polymer chain or in the benzene ring of the polymer matrix, do not depend on molecular conformation.

In Figure 7, it is also shown the experimental radial distribution function in the $\text{Diff}(r)$ form for compound **4**. The presence of MTO does not affect the long-range

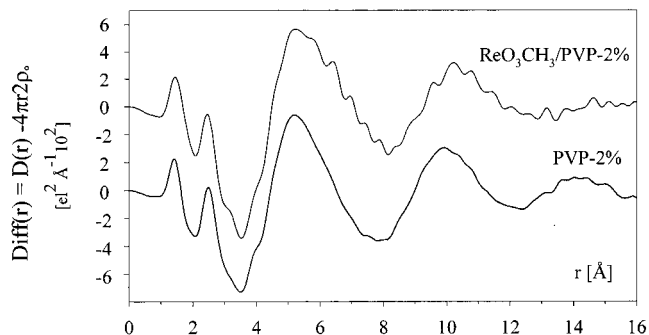


Figure 7. Experimental radial distribution functions in the $\text{Diff}(r) = D(r) - 4\pi r^2 \rho_0$ form: (a) $\text{ReO}_3\text{CH}_3/\text{PVP-2\%}$, (b) PVP-2\% .

polymer structure, but there are some minor differences in the main short-range peaks, due to the metal coordination sphere, which will be described in detail.

The structures of MTO in solid crystal state have been studied elsewhere.^{49,50} A complete structural study of the $\text{PVP-2\%}/\text{MTO}$ complex by X-ray diffraction would be very difficult and time-consuming. This is because the first coordination distances of the metal ions fall in the range of the second neighbors of the polymer. They are not dependent on amorphous resin structure, whereas the distances of the second and third coordination sphere are closely related to the resin structure. Thus, it would be necessary to determine the complete polymer structure in order to identify which atoms belong to the second coordination sphere of the metal.

We have assumed that MTO only induce minor modifications in the polymer structure because no substantial differences in the structure functions of PVP-2\% were detected. Thus, we are quite confident in the validity of the *difference method*. The difference method that was previously applied to the liquid systems, recently, was also applied to solid systems.⁴¹ In a liquid system, the addition of a small amount of solute to obtain a diluted solution does not alter its long- and medium-range structure. Thus, the solute–solute and solute–solvent interactions can be derived by subtracting the structure function of the solvent from that of the solution. In the present case, the PVP-2\% has been considered as a solvent. Therefore, we have subtracted a weighted amount of the experimental PVP-2\% structure function to the experimental curves of **4**. In so doing we can focus our attention on all new interactions present, namely MTO–polymer and MTO–MTO interactions. The use of the *difference method* was necessary because of the great complexity of the polymer structure and of the small proportion of MTO compared to the resin (0.5 loading factor).

We have subtracted the weighted PVP-2\% distribution radial function, $D(r)$ curve, Figure 8b, from the respective $D(r)$ curve of **4** (Figure 8, panel a). The resulting curve isolates the MTO–polymer and MTO–MTO interactions, and it is devoid of contributions of the polymer amorphous structure. The difference curves show three main peaks located at about 1.75, 2.35, and 3.20 \AA (Figure 8, panel b).

(49) Takacs, J.; Kiprof, P.; Riede, J.; Herrmann, W. A. *Organometallics* **1990**, *9*, 782–787.

(50) Romão, C. C.; Khün, F. E.; Herrmann, W. A. *Chem. Rev.* **1997**, *3197–3246*.

(48) *International Tables for X-ray Crystallography*; Kynoch Press: Birmingham, 1974; Vol. 4.

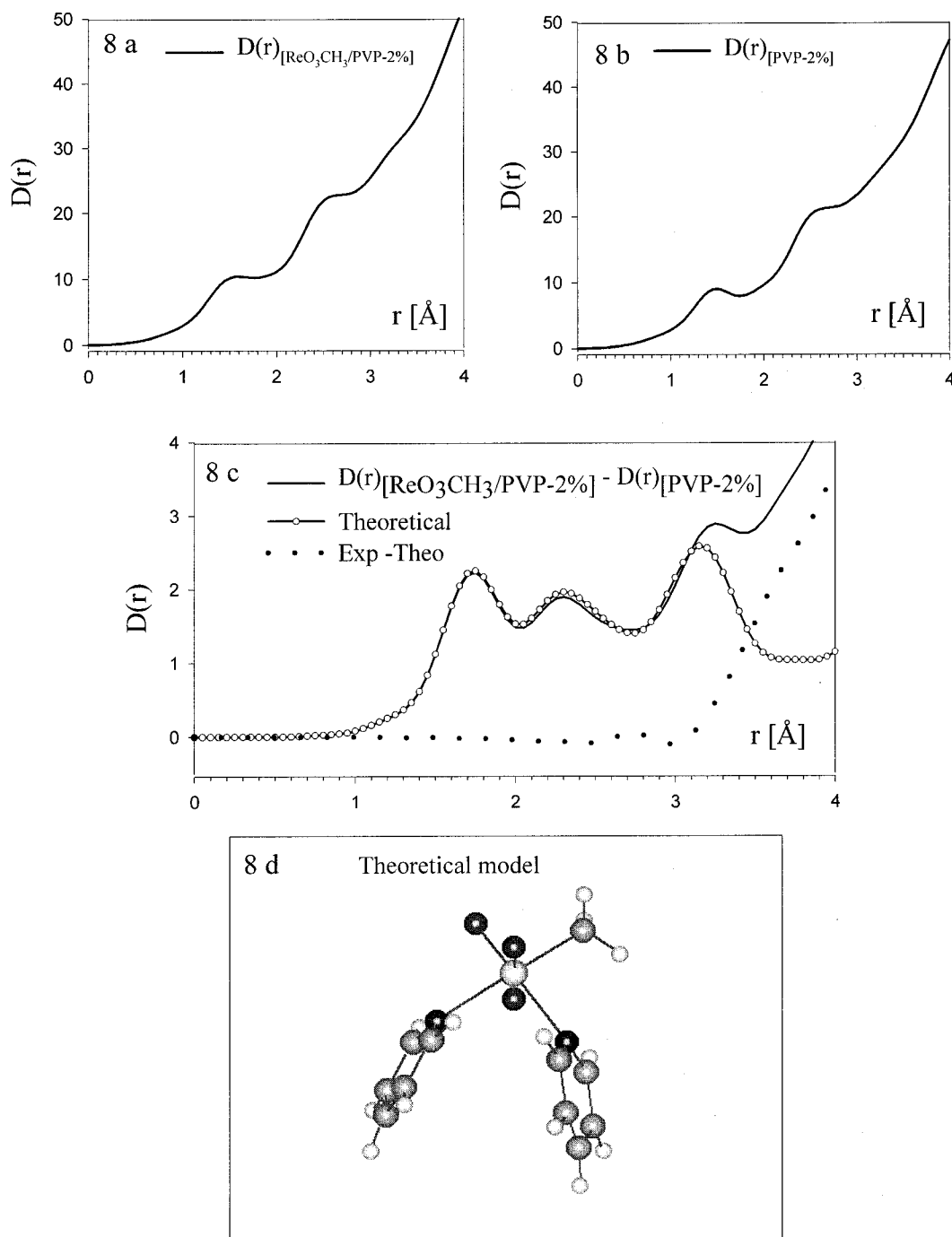


Figure 8. (a) Experimental radial distribution function $D(r)$ of $\text{ReO}_3\text{CH}_3/\text{PVP-2\%}$. (b) Weighted experimental radial distribution function $D(r)$ of PVP-2%. (c) Difference curve for the two radial distribution functions, $D(r)_{\text{ReO}_3\text{CH}_3/\text{PVP-2\%}} - D(r)_{\text{PVP-2\%}}$ [solid], theoretical molecular peak shapes for the shown model [red circle], difference curve for the radial distribution function and the theoretical molecular peak shapes [blue square]. (d) Balls and sticks view of the PVP-2% coordination to ReO_3CH_3 .

First, we analyzed the first peaks of the curves. They provide information on the metal's first neighbor interactions, i.e., on the bond distances, on the coordination numbers, and on the interaction types, metal–oxygen or metal–nitrogen. We found that the first peak at 1.75 Å was fitted by three metal–oxygen interactions, of 1.70 Å. The second peak is due to the interactions Re–N and Re–CH₃, which respectively fall at 2.35 and 2.10 Å. The experimental peak is fitted by two metal–nitrogen contributions and one metal–carbon. Six atoms assuming an octahedral conformation surround the metal. So far the interactions between the atoms belonging to the first coordination sphere of the metal contribute to the third

peak at 3.20 Å. The theoretical peak shape function for this model is compared with the experimental difference radial distribution function in Figure 8c.

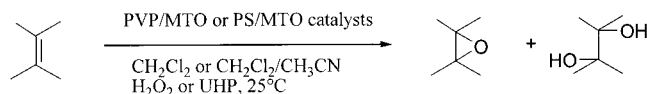
The values of the Re–O and Re–C bond distances found for **4** are in accord with the mean values previously reported for MTO/ L_n complexes.^{49,50} Thus, the Re–O and Re–C bond distances are nearly not influenced by the polymeric nature of the ligand. On the other hand, the Re–N bond distances were found abnormally shorter than that observed for MTO/ L_n complexes showing a strong coordination of the rhenium atom by the two nitrogens. The model presented in Figure 8 refers to one

Table 2. Distance (Å) of the Octahedral Arrangements of Re

Re-O1	1.70
Re-O2	1.70
Re-O3	1.70
Re-N1	2.35
Re-N2	2.35
Re-C	2.10

Table 3. Root Mean Square (rms) σ_{pq} Values Used in the Model of PVP-2%MTO 4

range (<i>r</i> , Å)	σ_{pq}
0 < <i>r</i> ≤ 2.00	0.050
2.00 < <i>r</i> ≤ 3.5	0.080
3.50 < <i>r</i> ≤ 7.00	0.150
7.00 < <i>r</i> ≤ 13.00	0.200
<i>r</i> > 13.00	0.300

Scheme 3

of the possible configurations that the coordinating atoms can take around the metal.

The distances between Re atom and ligands in octahedral arrangement are reported in Table 2

The same mean square deviation was assigned calculating the theoretical radial distribution function for each distance falling within a certain range, in the presented model. Five fixed root-mean-square values (rms σ_{pq}) were used. The σ_{pq} are given in Table 3

The analysis of the first coordination sphere of the metal does not allow us to determine the relative positions of the methyl group with respect to the oxygen and nitrogen atoms and of the oxygen and nitrogen atoms to each other. Besides, the two nitrogen atoms can belong to the same polymer chain or to two polymer chains. This analysis cannot discriminate the position of the methyl group because of the small electron differences between this group and the oxygen and nitrogen atoms. The analysis of the whole structure of the compound **4** can discriminate if one or two polymer chains are involved in the complex, and if the two nitrogen atoms are positioned perpendicular or parallel, one with respect to the other. The whole structure analysis of the complex **4** will be published elsewhere since it exceeds the scope of this work.

Polymer-Supported MTO-Catalyzed Epoxidation of Olefins. Epoxidations with hydrogen peroxide (H_2O_2) were investigated using *cis*-cyclohexene, *cis*-cyclooctene, styrene, α -methyl styrene, and *trans*-stilbene, as representative model substrates. As a general procedure, the olefin (1 mmol) to be oxidized and H_2O_2 (1.2 mmol, 30% aqueous solution) were added to a suspension of the catalyst (loading factor 0.5 or 1.0) in $\text{CH}_2\text{Cl}_2/\text{CH}_3\text{CN}$ (5 mL, 1:1 v/v), and the mixture was stirred at room temperature (Scheme 3). Catalysts were recovered by filtration at the end of the reaction after washing with CH_3CN and were used in successive oxidations under identical conditions (vide infra). In some cases the reaction was performed using urea/hydrogen peroxide adduct (UHP) as oxygen atom donor, and CH_2Cl_2 as solvent. In the absence of the catalyst, less than 2% conversion of substrates took place under otherwise identical conditions. Results are reported in Table 4. All poly(4-vinylpyridine)/MTO and polystyrene/MTO systems

Table 4. Poly(4-vinylpyridine)/MTO and Polystyrene/MTO Catalyzed Oxidation of Olefins^a

entry	olefin	catalyst	time (h)	conversion (%)	epoxide yield (%) ^b	1,2-diol yield (%) ^{b,c}
1	<i>cis</i> -cyclohexene	4	1.0	78	91	9
2	<i>cis</i> -cyclohexene	4/UHP^d	1.0	47	89	0
3	<i>cis</i> -cyclohexene	5	1.5	94	95	0
4	<i>cis</i> -cyclohexene	6	0.5	>98	82	18
5	<i>cis</i> -cyclohexene	4^e	0.5	80	>98	0
6	<i>cis</i> -cyclohexene	5^e	0.5	>98	>98	0
7	<i>cis</i> -cyclohexene	9	1.5	>98	55	45
8	<i>cis</i> -cyclooctene	4	0.5	>98	>98	0
9	<i>cis</i> -cyclooctene	5	0.5	>98	>98	0
10	<i>cis</i> -cyclooctene	6	0.5	96	>98	0
11	<i>cis</i> -cyclooctene	9	0.5	94	>98	0
12	styrene	4	2.0	>98	70	30
13	styrene	5	6.5	>98	>98	0
14	styrene	6	18	85	88	12
15	styrene	9	2.0	60	80	20
16	α -methylstyrene	4	12.0	95	75	25
17	α -methylstyrene	5	3.5	>98	>98	0
18	α -methylstyrene	6	7.0	>98	54	46
19	α -methylstyrene	9	1.0	>98	78	22
20	α -methylstyrene	9/UHP^d	2.0	68	>98	0
21	<i>trans</i> -stilbene	4	6.0	>98	46	54
22	<i>trans</i> -stilbene	5	6.0	>98	>98	0
23	<i>trans</i> -stilbene	6	1.0	>98	>98	0
24	<i>trans</i> -stilbene	9	1.0	93	>98	0

^a Under otherwise specified, all the reactions were performed in $\text{CH}_2\text{Cl}_2/\text{CH}_3\text{CN}$ (5 mL, 1:1 v/v) at room temperature, with H_2O_2 (30% aqueous solution), using a value of the catalyst loading factor of 1.0. ^b Refers to isolated materials. Yields normalized to 100% conversion. ^c No pinacol rearrangement products or products of other possible secondary reactions were observed by GC-MS and ¹H NMR spectrum of the crude reaction mixture. ^d Reaction performed in CH_2Cl_2 . ^e Loading factor 1.0.

Table 5. Stability of Poly(4-vinylpyridine)/MTO and Polystyrene/MTO Catalysts in the Epoxidation of *cis*-Cyclohexene^a

entry	catalyst	conversion (%) ^b				
		run no. 1	run no. 2	run no. 3	run no. 4	run no. 5
1	4	76(91) ^c	80(86)	74(83)	72(90)	75(92)
2	5	94(95)	91(>95)	89(92)	93(94)	95(93)
3	6	>98(82)	96(80)	94(81)	>98(81)	>98(84)
4	9	>98(55)	97(53)	95(54)	88(55)	77(53)

^a The reactions were performed in $\text{CH}_2\text{Cl}_2/\text{CH}_3\text{CN}$ (5 mL, 1:1 v/v) at room temperature, with H_2O_2 (30% aqueous solution), using a value of the catalyst loading factor of 1.0. ^b Determined by GLC analysis using a SPB column (25 m × 0.30 mm and 0.25 mm film thickness), and an isothermal temperature profile of 80 °C for the first 2 min, followed by a 10 °C/min temperature gradient to 200 °C for 10 min. ^c Values of the epoxide yield are given in parentheses and are normalized to 100% of conversion.

showed a high catalyst activity and selectivity for the formation of epoxides. Only in a few cases were *trans*-1,2-diols observed as side-products. The stability of the catalysts was determined, in some representative examples, by recycling experiments (Table 5).

The oxidation of *cis*-cyclohexene with the **4**/ H_2O_2 system gave cyclohexene oxide in acceptable conversion and yield, in the presence of a very low amount of *trans*-1,2-cyclohexanediol (Table 4, entry 1). As reported in Table 5 (entry 1), a slight decrease in activity occurred during five recycling experiments, showing that **4** is a stable catalyst.

This result is not completely in agreement with data previously reported by Herrmann and co-workers for the oxidation of *cis*-cyclohexene with heterogeneous MTO and

anhydrous H₂O₂ in *tert*-butyl alcohol, in which case only a low yield of epoxide (27%) was described (the conversion of the reaction and the yield of the diol are not reported by the authors).²⁴ A low conversion was obtained under similar experimental conditions using UHP as oxygen atom donor, and CH₂Cl₂ as solvent (Table 4, entry 2). In this case no traces of *trans*-1,2-diol were recovered by GC-MS and ¹H NMR spectrum of the crude reaction mixture. Probably, the heterogeneous character of UHP is responsible of the reduced activity of the catalyst. When the oxidation of *cis*-cyclohexene was performed with **5**, a high reaction conversion was obtained, and the epoxide was recovered in 95% yield (Table 4, entry 3). Note that with the poly(4-vinylpyridine) support, an enhancement of the reticulation-grade of the polymer increased both the efficiency and the selectivity of the reaction. Only a slight decrease in activity occurred during five recycling experiments (Table 5, entry 2). The oxidation of *cis*-cyclohexene with **6** and H₂O₂ showed a conversion higher than the previously obtained with **4**, a yield of epoxide higher than 80%, and an appreciable amount of diol as side-product (Table 4, entry 4). The role of pyridine *N*-oxide as mediator in the MTO-catalyzed epoxidation is still subject of a debate. It is well-known that the equilibrium constant for the interaction between pyridine *N*-oxide and MTO, determined by ¹H NMR analysis in CD₃NO₂, is of the same order ($K = 210 \pm 4 \text{ L mol}^{-1}$) than that recovered for pyridine ($K = 200 \pm 6 \text{ L mol}^{-1}$).⁵¹ Moreover, the pyridine *N*-oxide/MTO complex shows the highest value of the energy for the transition state in a frontal attack of the ligand-bisperoxo complex on ethylene as a model olefin (19.7 kcal mol⁻¹).²² At first glance, the pyridine-assisted epoxidation of olefins with MTO was found to be retarded by a large excess of pyridine, and this result was attributed to a detrimental effect of pyridine *N*-oxide on the stability of MTO.²³ On the other hand, Sharpless and co-workers showed that in the absence of olefin, MTO is an excellent and quite stable catalyst for the oxidation of pyridine.⁵¹ Thus, the low stability of the MTO in the pyridine-mediated system becomes relevant only in the presence of the olefin. In our case, **6** appears to be enough stable (Table 5, entry 3) to perform the epoxidation of *cis*-cyclohexene with high efficiency and selectivity. Even if we have not studied in detail the mechanism of the reaction, it is reasonable to suggest that the transition from an homogeneous system, pyridine *N*-oxide/MTO, to **6**, has a dramatic effect on the stability of the catalyst in the presence of the olefin.⁵²

In the oxidation of *cis*-cyclohexene with **4** and **5**, a modification of the loading factor of the catalyst from 0.5 to 1 displayed no particular advantages for the conversion and yield of epoxide, even if the reaction time was reduced to half (Table 4, entries 5 and 6). The microencapsulated system **9** showed a high activity, but a very low selectivity, and the *trans*-1,2-cyclohexanediol was recovered in almost 1:1 ratio with the epoxide (Table 4, entry 7). These data further confirm the importance of pyridine or pyridine *N*-oxide as Lewis base ligands to the rhenium atom for the selectivity of the epoxidation. Moreover, even if only a very slight decrease in activity occurs during the first four recycling experiments, in the fifth recycling step the conversion was appreciably re-

duced, probably because of a partial loss of MTO from the microcapsules (Table 5, entry 4).

In the oxidation of *cis*-cyclooctene, both poly(4-vinylpyridine)/MTO and polystyrene/MTO systems were shown to be active and selective catalysts. The conversions of the reactions were found always higher than 90%, and the cyclooctene oxide was the only recovered product (Table 4, entries 8–11).

To probe the generality of this procedure, we studied the synthesis of some sensitive epoxides, starting from styrene, α -methyl styrene, and *trans*-stilbene. The oxidation of styrene with **4** and **5** yielded the quantitative conversion of the substrate. Only **5** showed a high selectivity, while in the case of **4** the 1-phenyl-1,2-ethanediol was recovered in 30% yield (Table 4, entries 12 and 13). The same reaction performed with **6** and **9** as catalysts afforded the styrene oxide in acceptable conversion and yield. The diol was still obtained in 12% and 20% yields, respectively (Table 4, entries 14 and 15). A similar reaction pathway was observed for the high reactive α -methylstyrene, in which case **5** gave both a quantitative conversion and yield of α -methylstyrene oxide, while **4**, **6**, and **9** showed a high reactivity but not a similar high selectivity (Table 4, entries 16–19). Finally, the catalysts transformed the *trans*-stilbene into the corresponding epoxide with high conversion and selectivity, with the exception of **4**, in which case only a modest selectivity was obtained (Table 4, entries 21–24). It is important to note, that in the case of the catalysts based on the poly(4-vinylpyridine) as support, the self-oxidation of the free pyridine rings present on the polymer remains a potential problem. Sharpless and co-workers reported that the oxidation of alkenyl substituted pyridines shows a different reaction pathway if the alkenyl moiety is conjugated or not conjugated to the aromatic ring. In particular, in the case of conjugated pyridine derivatives, the *N*-oxidation pathway dominates and the corresponding epoxides were not detected. By contrast, the 4-(3'-cyclohexenyl)pyridine undergoes fast epoxidation while not *N*-oxidation was observed.³⁷ On the basis of these data, it is reasonable to suggest that in the oxidations of *cis*-cyclohexene and *cis*-cyclooctene, the self-oxidation of the PVP-2% and PVP-25% supports should not be an important side-process. On the other hand, with styrene, α -methylstyrene, and *trans*-stilbene, the largest reaction times were observed; thus, the possibility of the self-oxidation process cannot further ruled out. Regardless of whether or not the self-oxidation is a side process, Table 5 shows that PVP-2%/MTO and PVP-25%/MTO catalysts are stable enough to perform at least five recycling experiments with similar conversion and selectivity. Thus, if pyridine *N*-oxide moieties are formed, they did not interfere with the oxidation of the olefin at the rhenium active center.

Conclusions

Poly(4-vinylpyridine)/MTO and polystyrene/MTO systems are efficient and selective catalysts for the conversion of olefins to the corresponding epoxides, using environmentally friendly, easily available, and low cost H₂O₂ as oxygen atom donor. The efficient oxygen transfer activity of these systems, under relatively mild experimental conditions, may be attributed to the retained reactivity of the monoperoxo metal [MeRe(O)(O₂)] and a bisperoxo metal [MeRe(O)(O₂)₂] intermediates even in

(51) Wang, W.-D.; Espenson, J. H. *J. Am. Chem. Soc.* **1998**, *120*, 11335–11341.

(52) Copèret, C.; Adolfsson, H.; Khuong, T.-A. V.; Yudin, A. K.; Sharpless, K. B. *J. Org. Chem.* **1998**, *63*, 1740–1741.

the presence of the polymeric organic support. The UHP may be considered as an alternative to H_2O_2 for the synthesis of sensitive epoxides, even if lower reaction conversions are observed, probably because of the heterogeneous character of the oxidant. Independently from the system used in the oxidation, values of the loading factor of the catalyst higher than 0.5 did not give an appreciable increase of the reaction conversion or of the epoxide yield. Catalysts based on poly(4-vinylpyridine) are stable systems for at least five recycling experiments. By contrast, PS-2%/MTO showed a slight decrease in activity during the first four recycling experiments, while in the fifth recycling step the conversion was appreciably reduced. Thus, the physical envelopment of the benzene ring of polystyrene did not completely ensure the stability of the catalyst. In the case of PVP-2%/MTO the wide-angle X-ray diffraction (WAXS.) analysis performed by the application of the *difference method* showed the first reported geometry of a MTO heterogeneous species. The complex is characterized by a slightly distorted octahedral conformation on the metal's primary coordination sphere. The Re–O and Re–C bond distances are nearly not influenced by the polymeric nature of the ligand. On the other hand, the Re–N bond distances were found abnormally shorter than those observed for homogeneous MTO/ L_n complexes showing a strong coordination of the rhenium atom. These data are in accord with the high stability observed for this catalyst in recycling experiments. The reticulation grade of the polymer is a crucial factor for the catalysts based on poly(4-vinylpyridine), either for the morphology of the surface of particles and for the reaction pathway. Poly(4-vinylpyridine) 2% cross-linked systems, such as PVP-2%/MTO and PVPN-2%/MTO, are characterized by particles with irregular surfaces. On the other hand, the most reticulated PVP-25%/MTO shows particles with a regular spherical shape, the morphology of which is very similar to the microcapsules of PS-2%/MTO. Moreover, PVP-25%/MTO is the best catalyst system, giving the epoxides of conjugated and nonconjugated olefin derivatives in high conversions and yields. PVPN-2%/MTO, which is probably characterized by a pyridine *N*-oxide moiety as anchorage site for the rhenium atom, shows a reactivity and selectivity that is similar to that of PVP-2%/MTO, with the exception of conjugated olefin derivatives, in which cases a highest selectivity was observed. The loss of the detrimental effect of the pyridine *N*-oxide moiety on the stability of the catalyst, previously reported for the homogeneous system MTO/pyridine, is a new important clue. PS-2%/MTO is the less selective catalyst of all of the systems used. Design of other supported MTO compounds with high selectivity and activity is being undertaken in our laboratory.

Experimental Section

NMR spectra were recorded on a 200 MHz spectrometer and are reported in δ values. Infrared spectra were recorded on a FT-IR spectrophotometer using KBr and NaCl plates. Melting points were obtained on a Reichert Kofler apparatus and are

uncorrected. Gas chromatography and gas chromatography–mass spectroscopy (GC-MS) of the reaction products were performed using a SPB column (25m \times 0.30 mm and 0.25 mm film thickness) and an isothermal temperature profile of 80 °C for the first 2 min, followed by a 10 °C/min temperature gradient to 200 °C for 10 min. The injector temperature was 200 °C. Chromatography grade helium was used as the carrier gas. Mass spectra were recorded with an electron beam of 70 eV. For the scanning electron microscopy (SEM) photographs, samples were sputter-coated with gold (20 nm). Chromatographic purifications were performed on columns packed with silica gel, 230–400 mesh, for flash technique. All reagents and solvents were of highest grade commercially available and used purified or freshly distilled as required by literature procedures.

Preparation of Poly(4-vinylpyridine)/MTO Catalysts.

To a suspension of 600 mg of the appropriate resin in 4 mL of ethanol was added 77 mg (0.3 mmol) of MTO, and the mixture was stirred for 1 h using a magnetic stirrer. The solvent was removed by filtration, and the solid residue was washed five times with 20 mL of ethyl acetate each time and finally dried under high vacuum. Coocervates were found to envelop the solid core dispersed in the medium, and 5.0 mL of hexane were added to harden the capsule walls. The suspension was stirred for 1 h at this temperature and then slowly cooled to 0 °C. A yellow powder remained. In each case, MTO had completely become bound to the polymer. This result was confirmed by spectroscopic analysis of the residue obtained after evaporation of the organic layers. The catalyst was used without any further purification.

Preparation of Polystyrene/MTO Catalysts.

Polystyrene or the mixture poly(4-vinylpyridine)/polystyrene 600 mg (1:5 ratio) was suspended in 5.0 mL of THF at 25 °C, and to this solution was added 77 mg of MTO (0.3 mmol) as a solid core. The suspension was stirred for 1 h at this temperature and then slowly cooled to 0 °C. Coocervates were found to envelop the solid core dispersed in the medium, and 5.0 mL of hexane were added to harden the capsule walls. The mixture was stirred for 1 h at 25 °C. The solvent was removed by filtration, and the solid residue was washed five times with 20 mL of ethyl acetate each time and finally dried under high vacuum. A blue powder remained. In each case, MTO had completely become bound to the polymer. This result was confirmed by spectroscopic analysis of the residue obtained by evaporation of the organic layers. The catalyst was used without any further purification.

Oxidation of Olefins. General Procedure. To the suspension of 146 mg of the appropriate catalyst in 5.0 mL of $\text{CH}_3\text{CN}/\text{CH}_2\text{Cl}_2$ (ratio = 2 /1 v/v) at 25 °C were added the olefin (1 mmol) and the oxygen atom donor (2.0 mmol), H_2O_2 (2.0 mmol, 35% water solution), or urea hydrogen peroxide adduct (2.0 mmol, UHP). The reaction was monitored by gas chromatography, using dodecane as an internal standard. The suspension was filtered and the recovered catalyst washed five times with 10 mL of ethyl acetate each time. After drying under high vacuum, the catalyst was used for further reaction to evaluate its stability. The filtrate was treated with a low amount of manganese dioxide (MnO_2) at 25 °C to decompose the excess of primary oxidant and filtered. The solvent was dried with Na_2SO_4 . After the removal of the solvent, the crude product was analyzed by gas chromatography–mass spectroscopy and purified by preparative thin-layer chromatography to obtain the epoxides from acceptable to good yields. Products gave spectroscopic data consistent with the literature.